

## DISK EVOLUTION AND BAR TRIGGERING DRIVEN BY INTERACTIONS WITH DARK MATTER SUBSTRUCTURE

EMILIO ROMANO-DÍAZ<sup>1</sup>, ISAAC SHLOSMAN<sup>2,1</sup>, CLAYTON HELLER<sup>3</sup>, YEHUDA HOFFMAN<sup>4</sup>

*To be published by Astrophysical Journal Letters*

### ABSTRACT

We study formation and evolution of bar-disk systems in fully self-consistent cosmological simulations of galaxy formation in the  $\Lambda$ CDM WMAP3 Universe. In a representative model we find that the first generation of bars form in response to the asymmetric dark matter (DM) distribution (i.e., DM filament) and quickly decay. Subsequent bar generations form and are destroyed during the major merger epoch permeated by interactions with a DM substructure (subhalos). A long-lived bar is triggered by a tide from a subhalo and survives for  $\sim 10$  Gyr. The evolution of this bar is followed during the subsequent numerous minor mergers and interactions with the substructure. Together with intrinsic factors, these interactions largely determine the stellar bar evolution. The bar strength and its pattern speed anticorrelate, except during interactions and when the secondary (nuclear) bar is present. For about 5 Gyr bar pattern speed *increases substantially* despite the loss of angular momentum to stars and *cuspy* DM halo. We analyze the evolution of stellar populations in the bar-disk and relate them to the underlying dynamics. While the bar is made mainly of an intermediate age,  $\sim 5 - 6$  Gyr, disk stars at  $z = 0$ , a secondary nuclear bar which surfaces at  $z \sim 0.1$  is made of younger,  $\sim 1 - 3$  Gyr stars.

*Subject headings:* cosmology: dark matter — galaxies: evolution — galaxies: formation — galaxies: halos — galaxies: interactions — galaxies: kinematics and dynamics

### 1. INTRODUCTION AND NUMERICS

Within the framework of structure formation in the universe, a hierarchy of dark matter (DM) masses form, while baryons assemble in their midst as galactic disks (e.g., White & Rees 1978). Disk evolution is expected to be influenced heavily by mergers and interactions in various ways. In this Letter, we focus on the specific issue of a tidal triggering of stellar bars embedded in a disk and surrounded by a DM halo with a substructure, within the context of cosmological evolution in the WMAP3 universe (see also Dubinski et al. 2008). We analyze the dynamical aspects of this evolution and follow the prevailing stellar populations in the bar-disk system.

Recent efforts to understand galaxy formation have been spearheaded by the work on pure DM halo formation (e.g., Diemand et al. 2007) and associated disk growth (e.g., Sommer-Larson et al. 2003; Governato et al. 2004, 2007; Heller et al. 2007a,b). Addition of baryonic component(s) to this modeling has met with difficulties, partly due to a numerical resolution, star formation (SF), energy feedback, and other processes. Dissipation is relatively slow in disks, but can be accelerated by any substantial departure from axial symmetry due to gravitational torques — a nonlocal viscosity, surpassing the conventional viscosity by orders of magnitude. Torques facilitate the redistribution of mass, angular momentum and energy between the disk baryons and the slowly tumbling DM halo. Two main sources can serve as triggers of gravitational torques onto the disk — an asymmetric

mass distribution in the DM halo, and its non-uniformity, i.e., substructure, in DM and baryons. Both tidal interactions (e.g., Byrd et al. 1986; Noguchi 1987; Gerin et al. 1990) and DM halo asymmetry (Heller et al. 2007a,b) are likely to trigger stellar bars. About 1/3 of the large-scale bars host additional nuclear bars (Laine et al. 2002; Erwin & Sparke 2002).

Observations and numerical simulations point to an intricate relation between the stellar populations and the underlying dynamics of bars (e.g., Martin & Friedli 1997; Knapen et al. 1995a,b; Jogee et al. 2002a,b; Zurita & Perez 2008). For bars in a cosmological context, this issue becomes even more relevant, because the disk is open to accretion of cold gas and energy input from interactions. Here we attempt to answer some questions about the long-term evolution of bar-disk populations and relate it to the dynamical history of the system.

So far, nearly all modeling of bar evolution has been limited to isolated systems in a stationary state, with the exception of simulations of tidal interactions in controlled experiments (e.g., Gauthier et al. 2006). We test the bar origin and evolution in the cosmological setting without fine-tuning and minimizing the prior assumptions.

Numerical simulations have been performed using the FTM-4.5 hybrid  $N$ -body/SPH code (e.g., Heller & Shlosman 1994; Heller et al. 2007b; Romano-Díaz et al. 2008a) using physical coordinates. The total number of DM particles is  $2.2 \times 10^6$  and the SPH particles  $4 \times 10^5$ . The gravity is computed using the falCON routine (Dehnen 2002) which scales as  $O(N)$ . The gravitational softening is 500 pc, for DM, stars and gas. We assume the  $\Lambda$ CDM cosmology with WMAP3 parameters,  $\Omega_m = 0.24$ ,  $\Omega_\Lambda = 0.76$  and  $h = 0.73$ , where  $h$  is the Hubble constant in units of  $100 \text{ km s}^{-1} \text{ Mpc}^{-1}$ . The variance  $\sigma_8 = 0.76$  of the density field convolved with the top hat window of radius  $8h^{-1} \text{ Mpc}$  is used to normalize

<sup>1</sup> Department of Physics and Astronomy, University of Kentucky, Lexington, KY 40506-0055, USA

<sup>2</sup> JILA, University of Colorado, Boulder, CO 80309, USA

<sup>3</sup> Department of Physics, Georgia Southern University, Statesboro, GA 30460, USA

<sup>4</sup> Racah Institute of Physics, Hebrew University; Jerusalem 91904, Israel

the power spectrum. The SF algorithm is described in Heller et al. (2007b). We note only that multiple generations of stars can form from a single SPH particle. The energy and momentum feedback into the ISM are implemented, and the associated parameters have the following values (Heller et al.): energy thermalization  $\epsilon_{\text{SF}} = 0.3$ , cloud gravitational collapse  $\alpha_{\text{ff}} = 1$ , and self-gravity fudge-factor  $\alpha_{\text{crit}} = 0.5$ .

Initial conditions generated here are those of Romano-Diaz et al. (2008a): we use the Constrained Realizations (CR) method (Hoffman & Ribak 1991) within a restricted box size of  $8h^{-1}$  Mpc and a sphere of  $5h^{-1}$  Mpc is carved out and evolved. A large-scale filament runs across the computational sphere and is banana-shaped. The constructed Gaussian field is required to obey a set of constraints of arbitrary amplitudes and positions (more about this method in Romano-Diaz et al. 2006, 2007). Two constraints were imposed on the density field, first — that the linear field Gaussian smoothed with a kernel of  $1.0 \times 10^{12} h^{-1} M_{\odot}$ , has an over-density of  $\delta = 3$  at the origin ( $2.5\sigma$  perturbation, where  $\sigma^2$  is the variance of the appropriately smoothed field). It was imposed on a  $256^3$  grid and predicted to collapse at  $z_c \sim 1.33$  based on the top-hat model. This perturbation is embedded in a region (2nd constraint) corresponding to a mass of  $5 \times 10^{13} h^{-1} M_{\odot}$  in which the over-density is zero, i.e., the unperturbed universe. The random component in CRs favors formation of similar structures which leads to major mergers. The DM mass inside the computational sphere is  $\sim 6.1 \times 10^{12} h^{-1} M_{\odot}$ . We have randomly replaced 1/6 of DM particles by equal mass SPH particles. Therefore,  $\Omega_{\text{m}}$  is not affected.

## 2. EVOLUTION AND STELLAR POPULATIONS

The prime halo evolves through a series of major mergers which end by  $z \sim 1.5$ , while accretion of subhalos and smooth accretion continue to the present, mainly along the filament. The number of subhalos varies with time, and at its peak is about few hundred, for subhalos in excess of  $10^8 M_{\odot}$ . The disk is recognizable from  $z \sim 8$ , associated with a strong SF. It grows from inside out and appears strongly non-axisymmetric and barred along the filament. The first merger of nearly equal masses is gas-rich, coplanar and prograde. The disk reforms immediately, although the bar does not ( $z \sim 5$ ). Next merger, at  $z \sim 4$ , is again prograde and excites a bar which is destroyed shortly. Subsequent minor mergers drive a strong spiral structure, as the disk grows to  $\sim 10$  kpc, and push the gas inwards in a ‘shepherding’ mode. The SF is vigorous in the high surface density gas. At  $z \sim 2.6$ , the tide from a subhalo (prograde and inclined penetrating minor merger) triggers a strong gas-rich bar (Fig. 1) followed by (minor) merger activity till  $z = 0$ . A direct hit by another disk (in a host subhalo), on  $\sim 40^\circ$ -inclined prograde trajectory, weakens the bar abruptly at  $z \sim 2.2$  and shortens it. A retrograde encounter at  $z \sim 1.4$  has no dramatic effect on the bar. As a result of these interactions the gas-rich disk shrinks gradually. Overall, the disk axis is oriented along the halo minor axis, but this orientation experiences strong departures during the major merger epoch. The DM halo forms an isothermal cusp,  $R^{-2}$ , within 15 kpc which survives beyond  $z \sim 1$  and is ultimately washed out, leaving a flat core of  $\sim 2 - 3$  kpc (Romano-Diaz et al. 2008b).

Bar dynamics is displayed in Fig. 2. The pattern speed,  $\Omega_{\text{b}}$ , of the initial barlike response to the DM stagnates initially, then accelerates. The bar amplitude,  $A_2$  of the  $m = 2$  Fourier mode, decays rapidly. The oval perturbation in the stellar disk remains but is weak and noisy, and therefore omitted here until the tidal triggering at  $z \sim 2.6$ . Subsequent evolution depends both on interactions with the substructure and on intrinsic factors.

For the newly triggered bar,  $\Omega_{\text{b}}(z)$  largely anticorrelates with  $A_2(z)$ . Amazingly, it increases over  $\sim 5$  Gyr until the peak at  $z \sim 0.8$ , when  $\Omega_{\text{b}}$  starts a sharp decay.  $\Omega_{\text{b}}(z)$  experiences a break at  $z \sim 0.35$  and becomes shallower, while the bar weakens abruptly (minor merger). This evolution is analyzed in §3.

To view the evolution of stellar populations in the bar and the surrounding disk, we have separated the stars into age groups: 5–6 Gyrs, 3–4 Gyrs, 2–3 Gyrs, 1–2 Gyrs, 0–1 Gyrs and 0–0.03 Gyrs old. These are shown via frames at  $z = 0.3$  and  $z = 0$  for face-on (Fig. 3) and edge-on (Fig. 4) disks.

Division into populations reveals certain aspects of the internal dynamics in the disk. The older stellar population of 5-6 Gyr dominates the disk and bar masses, and the ongoing SF is peaked at the center at  $z = 0$ . Figs. 3 and 4 display colors based on stellar ages. The bar has a prominent rectangular shape only when observed face-on in 1–3 Gyr old stars at  $z = 0.3$ . This means that the bar extends to the ultra-harmonic resonance and its outer part is populated by stars which are trapped by the characteristic 4:1 orbits.

A nuclear bar emerges after  $z \sim 0.1$  (Fig. 3) for 0–3 Gyr aged stars at  $z = 0$ . One can understand the appearance of this morphology because the prime bar slows down substantially (Fig. 2) and this leads to an inner Lindblad resonance (ILR). A new family of periodic orbits forms inside this resonance and these orbits are known to be elongated normal to the orbital family which supports the main bar figure. This new family of orbits is populated by stars with the lowest dispersion velocities, i.e., the youngest stars inside the ILR because the trapping ability of the nuclear bar is low.

## 3. DISCUSSION: DYNAMICS AND POPULATIONS

We have studied the evolution of galactic bars in fully self-consistent cosmological simulations of galaxy formation. In a representative model, we find that the first generation of bars forms early and in response to the asymmetric background DM distribution. This bar decays quickly and subsequent bars form and are destroyed by interactions with subhalos. Finally, a long-lived bar is triggered that survives for  $\sim 10$  Gyr. Most interestingly, its pattern speed *increases substantially* over the first  $\sim 5$  Gyr, despite the angular momentum loss to the outer disk and the cuspy DM halo. The bar evolution appears to be closely linked to the disk evolution — it is permeated by interactions with subhalos as we discuss below.

The sequence of bars in the model are repeatedly triggered by interactions with DM substructure and do not form as a result of a ‘classical’ (i.e., intrinsic) bar instability. The number of subhalos within the inner prime halo is highly variable — the subhalos cluster in the filament and are frequently accreted in groups before they merge (Romano-Diaz et al. 2008b). This amplifies the dam-

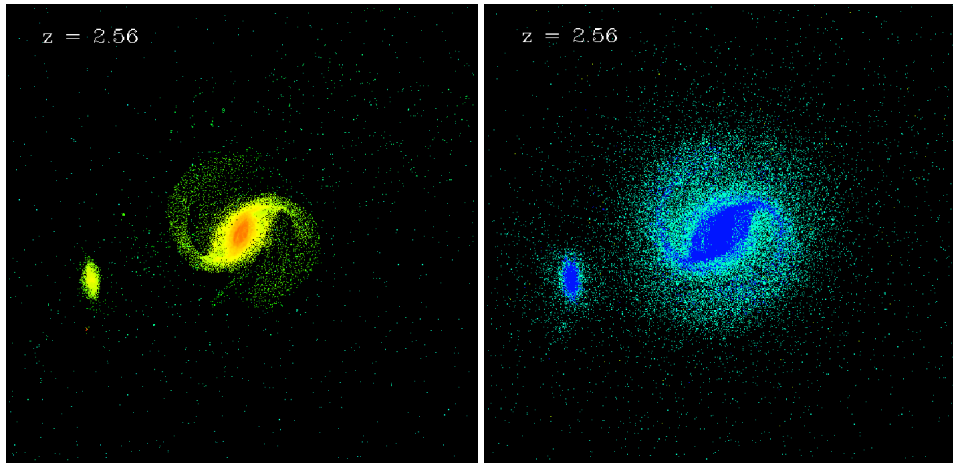


FIG. 1.— Penetrating minor merger triggering gas-rich stellar bar in the growing disk. The intruder is on the prograde trajectory inclined to the disk plane by about  $50^\circ$  with an impact parameter of  $\sim 9$  kpc. *Left*: gas; *Right*: stars — the color palette traces the stellar ages (0–0.2 Gyr blue; 0.2 – 2 Gyr aquamarine). The intruder is also gas rich and is shown near the closest first approach.

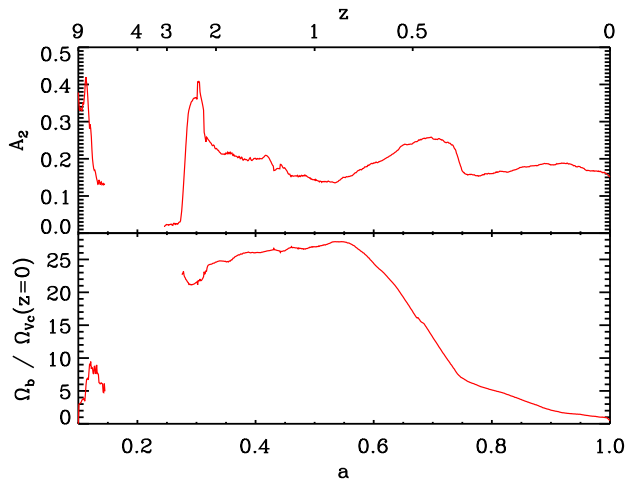


FIG. 2.— Evolution of the bar amplitude  $A_2$  (upper) and pattern speed  $\Omega_b$  (lower) with the cosmological expansion factor  $a$  and redshift  $z$ . The gap corresponds to a particularly intensive merger activity when both curves are ill-defined.  $\Omega_b$  is normalized by the angular velocity of a test particle at the radius of a maximal rotation velocity in the halo at  $z = 0$ . The first generation bar (during the first Gyr) is induced by the main DM filament, while the next generations are tidally-induced and destroyed. Finally, a long-lived bar is tidally triggered by the interaction with a subhalo in a highly-inclined prograde encounter (Fig. 1).

age inflicted by the substructure on the disk-bar system because of higher mass and energy influx into the disk region. We find that the prograde encounters trigger bars, direct hits weaken existing bars, while retrograde encounters have little effect — in line with Gerin et al. (1990) and Berentzen et al. (2004). In spite of this, addition of the cold gas to the disk, up to  $R \sim 15$  kpc, in tandem with growing stellar surface density by  $\sim 10$ , allow the bar to speed up over  $\sim 5$  Gyr (Fig. 2). This happens because the buildup of a disk mass and the increased central mass concentration in the galaxy amplifies the precession rate of bar orbits. On the other hand, the weakening of the bar during this time results from the angular mo-

mentum added by the gas to the disk and, therefore, to the bar. This happens because orbits trapped within the bar become less eccentric, leading to a weaker bar.

The gas fraction in the disk exceeds that considered so far in the literature by as much as a factor of 10 (Bournaud et al. 2005; Berentzen et al. 2007). It is an influx of subhalos into the center which strips the disk of its gas and heats up the stellar ‘fluid’ injecting it above the plane. Being cut off from the source of angular momentum, the bar brakes rapidly.

An important caveat of this slowdown is the bar weakening after  $z \sim 0.1$  (Fig. 2). Here we do not observe the anticorrelation between  $A_2$  and  $\Omega_b$ . The appearance of the nuclear bar sheds light on this behavior. The orbit trapping by the nuclear bar which grows due to a slowdown deprives the main bar of orbital support — the weakening of the main bar and the strengthening of the nuclear bar proceed in tandem.

Stellar populations provide a further insight into the dynamics of the bar-disk systems. When viewed in colors of a younger stellar population, the disk is thinner and shows less contribution to the spheroidal component. Comparison of the left frames in Fig. 4 also shows that the spheroidal component is populated by stars older than the average disk population, as it disappears in the lower frame.

An interesting feature is present in  $z = 0$  frames of Fig. 4 with stars younger than 4 Gyr in the center — the upper/lower surfaces are flat and parallel to the disk midplane. It is associated with the vertical oscillations of stars in the region, and closely resembles the boxy bulges observed in about 50% of edge-on disk galaxies (e.g., Lutticke et al. 2000). These bulges originate in trapping by a family of 3-D orbits belonging to the prime bar (e.g., Combes et al. 1990; Skokos et al. 2002; Martinez-Valpuesta et al. 2006).

The SF continues after the major merger epoch,  $z \lesssim 1.5$  (Fig. 5). The asymptotic value for the SF rate,  $\text{SFR} \sim 1 M_\odot \text{ yr}^{-1}$ , in the disk was not fine-tuned but results from self-regulation. Early SF is supported by the cold gas accretion onto the disk. In the later stage, the SF is limited to the central kpc only — this explains the

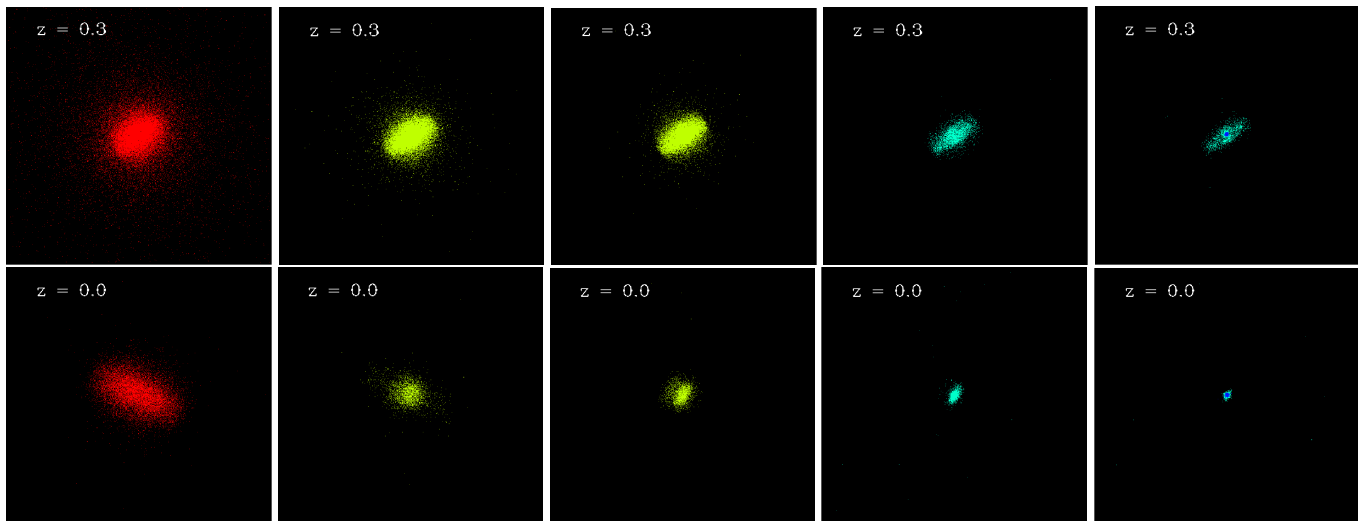


FIG. 3.— Stellar populations of the face-on disk divided into age groups at  $z = 0.3$  (upper) and  $z = 0$  (lower). From left to right the ages are: 5–6 Gyr, 3–4 Gyr, 2–3 Gyr, 1–2 Gyr and 0–1 Gyr. The right frames also include the subgroup of 0–0.03 Gyr old stars. Note the appearance of a *nuclear bar* oriented at  $90^\circ$  with respect to the main bar at  $z = 0$  and visible for stars younger than  $\sim 3$  Gyr (lower frames). Frames: 17 kpc on the side.

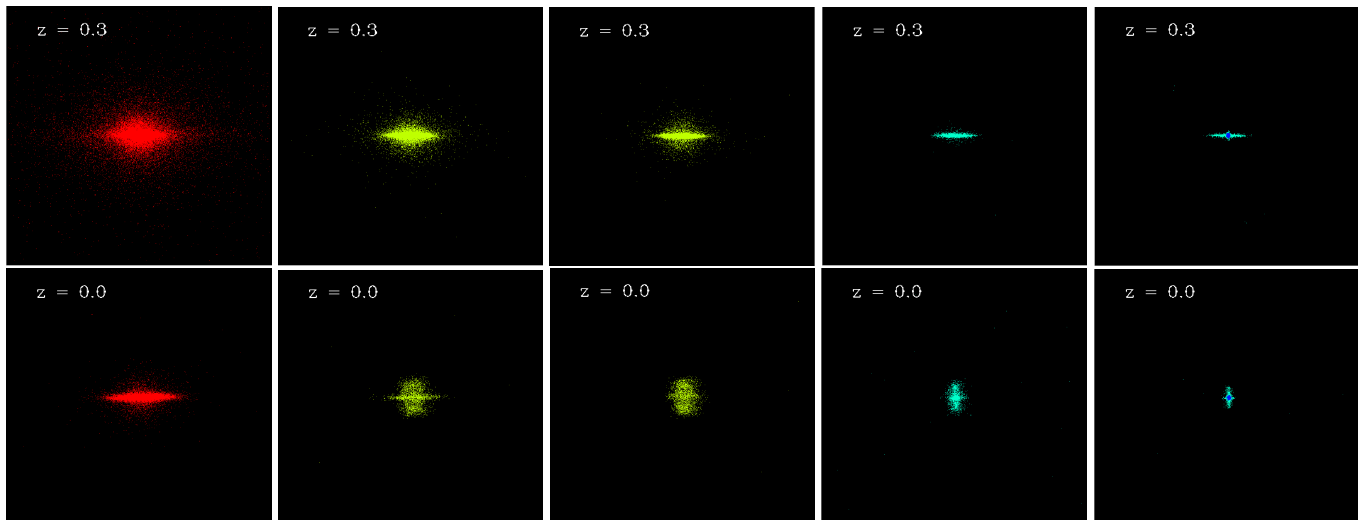


FIG. 4.— Same as Fig. 3 but for an edge-on disk.

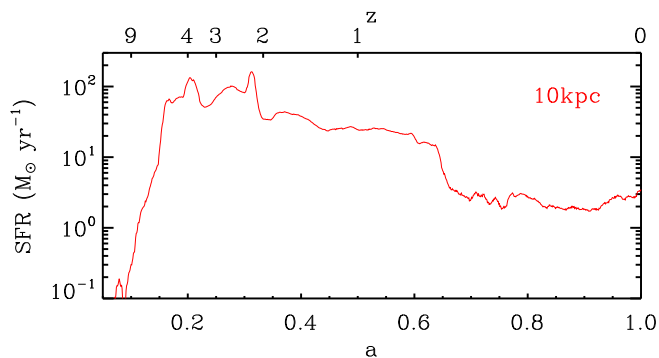


FIG. 5.— SF rates shown within the inner 10 kpc of the disk.

stellar age gradient in the disk which is positive (Figs. 3, 4). The bar resembles those in the early type galaxies with a constant surface brightness along the bar major axis, unlike the exponential bars which show negative age gradients (Perez et al. 2007).

In summary, we have followed the bar evolution in the most realistic environment attempted so far. We have shown that bars can maintain their fast rotation for  $\sim 5$  Gyr despite the loss of angular momentum to the disk and *cuspy* DM halo. Finally, bar dynamics appears to be closely linked to the disk stellar populations.

We are grateful to our colleagues, and especially to John Dubinski, Shardha Jogee, Seppo Laine, Irina Marinova, Reynier Peletier and Jorge Villa-Vargas for discussions and comments. This research has been partially

supported by NASA and STScI.

## REFERENCES

- Berentzen, I., Athanassoula, E., Heller, C.H., Fricke, K.J. 2004, MNRAS, 347, 220
- Berentzen, I., Shlosman, I., Martinez-Valpuesta, I. & Heller, C.H. 2007, ApJ, 666, 189
- Bournaud, F., Combes, F. & Semelin, B. 2005, MNRAS, 364, L18
- Byrd, G.G., Valtonen, M.J., Valtaoja, L. & Sundelius, B. 1986, A&A, 166, 75
- Combes, F., Debbasch, F., Friedli, D. & Pfenniger, D. 1990, A&A, 233, 82
- Dehnen, W. 2002, J. Comput. Phys., 179, 27
- Diemand, J., Kuhlen, M. & Madau, P. 2007, ApJ, 667, 859
- Dubinski, J., Gauthier, J.-R., Widrow, L. & Nickerson, S. 2008, Formation & Evolution of Disk Galaxies, ASP Conf. Ser., J.G. Funes & E.M. Corsini (eds.), astro-ph/0802.3997
- Erwin, P. & Sparke, L.S. 2002, AJ, 124, 65
- Gauthier, G.-R., Dubinski, J. & Widrow, L. 2006, ApJ, 653, 1180
- Gerin, M., Combes, F. & Athanassoula, E. 1990, A&A, 230, 37
- Governato, F., et al. 2004, ApJ, 607, 688
- Governato, F., et al. 2007, MNRAS, 374, 1479
- Heller, C.H. & Shlosman, I. 1994, ApJ, 424, 84
- Heller, C.H., Shlosman, I. & Athanassoula, E. 2007a, ApJ, 657, L65
- Heller, C.H., Shlosman, I. & Athanassoula, E. 2007b, ApJ, 671, 226
- Hoffman, Y. & Ribak, E. 1991, ApJ, 380, L5
- Jogee, S., Knapen, J.H., Laine, S., Shlosman, I., Scoville, N.Z. & Englmaier, P. 2002a, ApJ, 570, L55
- Jogee, S., Shlosman, I., Laine, S., Englmaier, P., Knapen, J.H., Scoville, N.Z. & Wilson, C.D. 2002b, ApJ, 575, 156
- Knapen, J.H., Beckman, J.E., Shlosman, I., Peletier, R.F., Heller, C.H. & de Jong, R.S. 1995a, ApJ, 443, L73
- Knapen, J.H., Beckman, J.E., Heller, C.H., Shlosman, I. & de Jong, R.S. 1995b, ApJ, 454, 623
- Laine, S., Shlosman, I., Knapen, J.H. & Peletier, R.F. 2002, ApJ, 567, 97
- Lütticke, R., Dettmar, R.-J. & Pohlen, M. 2000, A&AS, 145, 405
- Martin, P. & Friedli, D. 1997, A&A, 326, 449
- Martinez-Valpuesta, I., Shlosman, I. & Heller, C.H. 2006, ApJ, 637, 214
- Noguchi, M. 1987, MNRAS, 228, 635
- Perez, I., Sanchez-Blazquez, P. & Zurita, A. 2007, A&A, 465, L9
- Romano-Diaz, E., Hoffman, Y., Heller, C.H., Faltenbacher, A., Jones, D. & Shlosman, I. 2006, ApJ, 637, L93
- Romano-Diaz, E., Hoffman, Y., Heller, C.H., Faltenbacher, A., Jones, D. & Shlosman, I. 2007, ApJ, 657, 56
- Romano-Diaz, E., Shlosman, I., Heller, C.H. & Hoffman, Y. 2008a, ApJ, submitted
- Romano-Diaz, E., Shlosman, I., Hoffman, Y. & Heller, C.H. 2008b, ApJLett., in press, October 1 issue, arXiv:0808.0195
- Skokos, Ch., Patsis, P.A. & Athanassoula, E. 2002, MNRAS, 333, 847
- Sommer-Larsen, J., Götz, M., Portinari, L. 2003, ApJ, 596, 47
- White, S.D.M. & Rees, M.J. 1978, MNRAS, 183, 341
- Zurita, A. & Perez, I. 2008, A&A, 485, 5